VENTILATORY MODES AND MECHANICS OF THE HEDGEHOG SKATE (*LEUCORAJA ERINACEA*): TESTING THE CONTINUOUS FLOW MODEL

ADAM P. SUMMERS[1],* AND LARA A. FERRY-GRAHAM[2],‡

[1]*Museum of Vertebrate Zoology and Department of Integrative Biology, University of California, Berkeley, CA 94720, USA* and [2]*Comparative Physiology Group, Department of Ecology and Evolution, University of California, Irvine, CA 95697, USA*

*e-mail: summers@uclink.berkeley.edu
‡Present address: Center for Population Biology and Section of Evolution and Ecology, University of California, Davis, CA 95616, USA

Summary

The movement of water across the gills of non-ram-ventilating fishes involves the action of two pumps: a pressure pump that pushes water across the gills from the oropharyngeal to the parabranchial cavity, and a suction pump that draws water across the gills from the oropharyngeal into the parabranchial cavity. Together, the two are thought to keep water flowing continuously antero-posteriorly through the head of the respiring animal. However, there is evidence that the pressure and suction pumps do not always work in perfect phase in elasmobranch fishes, leading to periods of higher pressure in the parabranchial than in the oropharyngeal cavity. We investigated the existence and consequence of such pressure reversals in the hedgehog skate *Leucoraja erinacea* using pressure transducers, sonomicrometry and flow visualization including internal visualization using endoscopy. We noted four patterns of respiration in the experimental skates distinguished by the flow pattern at the three openings into the respiratory system: (1) in through the spiracle only, (2) in through the mouth + spiracle, (3) in through the mouth only, and (4) the mouth held open throughout the respiratory cycle. The first two were by far the dominant modes recorded from experimental animals. We determined that pressure reversals exist in the hedgehog skate, and that the gill bars adducted during such pressure reversals. Direct observation confirmed that these pressure reversals do correspond to pulsatile flow across the gills. During mouth+spiracle ventilation the flow completely reversed direction, flowing from the parabranchial chambers back across the gills and into the oropharyngeal cavity. Finally, we addressed the utility of sonomicrometry as a technique for determining kinematics in aquatic animals. Despite some problems involving errors inherent to the system design, we found the technique useful for complementing such techniques as pressure measurements and endoscopy.

Key words: hedgehog skate, *Leucoraja erinacea*, gill ventilation, continuous flow model, pressure reversal, sonomicrometry, flow visualization.

Introduction

Aquatic respiration in many fishes is a mechanical ballet in which water is pumped from the oropharyngeal chamber, across the gills and into the parabranchial chambers. At the same time, blood is pumped through the gills, where it picks up oxygen from the water and loses carbon dioxide. The movement of water across the gills involves the action of two pumps: a pressure pump that pushes water across the gills from the oropharyngeal to the parabranchial cavity, and a suction pump that draws water across the gills from the oropharyngeal into the parabranchial chamber (Hughes and Morgan, 1973). A synchrony between these two pumps can theoretically yield a continuous flow of water across the gills in spite of discontinuous flow into the mouth and out of the gill slit(s). The blood flow in the respiratory structures of the gills (secondary lamellae) is in the opposite direction to that of water (Grigg and Read, 1971; Scheid and Piiper, 1976).

The continuous flow of water across the gills requires two cyclical pumps; one must be active while the other is refilling. The buccal pressure pump is clearly present in all fishes; however, the suction pump is not. In the bony fishes (Osteichthyes), abduction of the operculum serves as the suction pump (Hughes, 1960b; Hughes and Shelton, 1958). It is less obvious in cartilaginous fishes (Chondrichthyes) where the motive force for the suction pump comes from, although the elastic recoil of the branchial skeleton and small muscles that extend the elements of the gill arch may be responsible (Hughes and Ballintijn, 1965). Flow is difficult to measure inside a fish's head, so relative pressures in the oropharyngeal and parabranchial (or opercular) cavities have been used as an indicator of flow direction. In experiments on bony and cartilaginous fishes, these measures of pressure have been used to indicate that the dominant flow pattern is a continuous,

unidirectional flow across the gills (Ballintijn, 1969; Ballintijn, 1972; Hughes, 1960a; Hughes and Shelton, 1958). An extensive body of literature modeling the movement of gases and ions across the gills has been predicated on these two assumptions: (i) that the flow is continuous, and (ii) that the flow is counter-current with respect to the flow of blood through the capillaries of the gill (for reviews, see Piiper, 1998; Piiper and Scheid, 1984).

However, there is evidence that the pressure and suction pump do not always work in perfect phase, leading to periods of higher pressure in the parabranchial than the oropharyngeal cavity (Ferry-Graham, 1999; Hughes, 1960a; Hughes and Morgan, 1973). This pressure differential, a reversal of the normal pressure profile, may mean that water sometimes flows back across the gills and into the oropharyngeal cavity. In other words, for some portion of the respiratory cycle, the water flow is co-current with the blood flow rather than counter-current. This would necessitate

changes to the models of gas exchange. Pressure reversals, although perhaps not flow reversals, may be widespread among fishes and are clearly seen in experiments on two species of shark (Ferry-Graham, 1999; Hughes, 1960a). Pressure reversals need not be equivalent to flow reversals because active closure of a valve between the two chambers could allow a pressure differential with no back-flow. The gill bars lie between the two chambers and have appropriate musculature to adduct during pressure reversals, as they do during suction generation for feeding (Lauder, 1980).

The question of the relationship between oropharyngeal pressure, parabranchial pressure and flow can be resolved directly by visualizing the water flow and indirectly by examining the kinematics of the gill bars and other important structures. Water flow can be directly visualized with an endoscope (Sanderson et al., 1996) led into the head through a small cannula. Small particles in the water flow at the same speed as the water itself. To visualize the position of
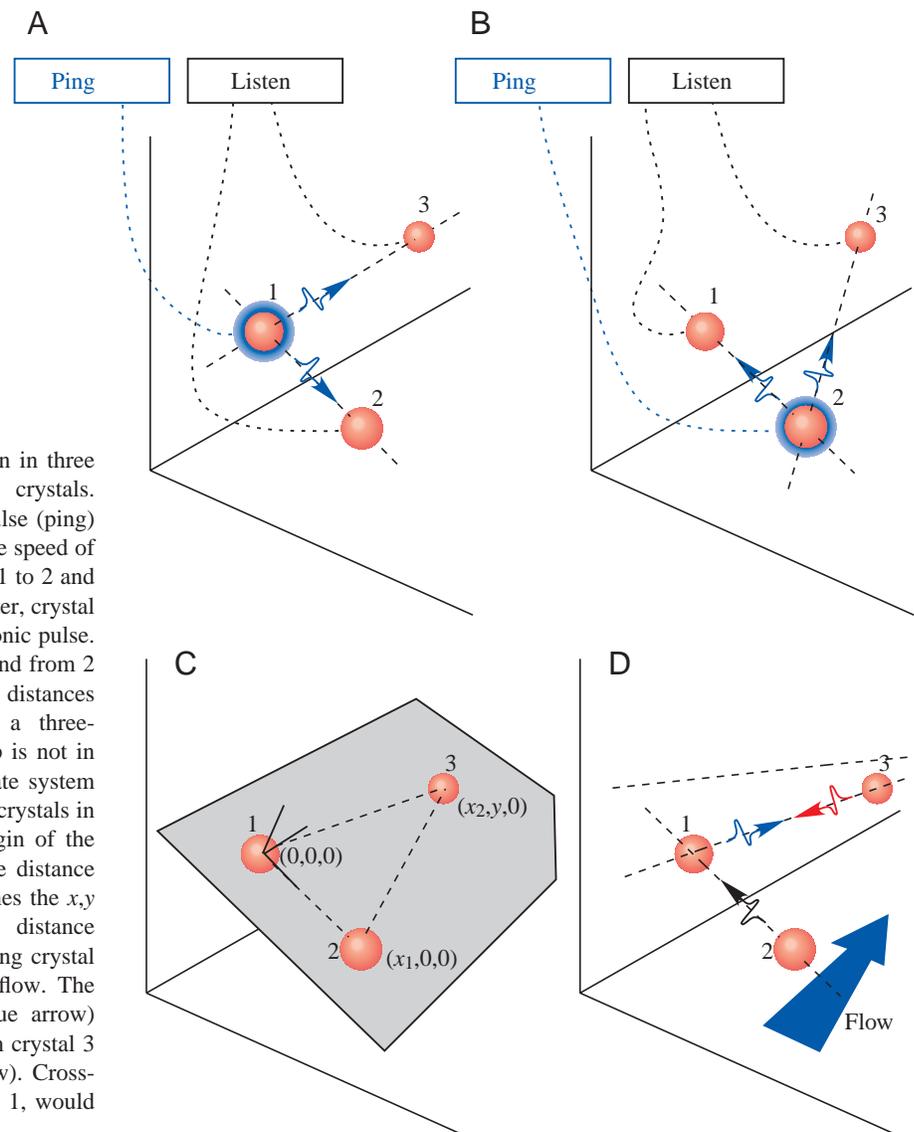

Fig. 1. An illustration of position determination in three dimensions by multiplexed sonomicrometry crystals. (A) Crystal 1 sends out an ultrasonic sound pulse (ping) which is heard by crystals 2 and 3. Knowing the speed of sound in the medium allows the distance from 1 to 2 and from 1 to 3 to be determined. (B) Some time later, crystal 2 pings and crystals 1 and 3 receive that ultrasonic pulse. Again, distance can be computed from 2 to 1 and from 2 to 3. (C) By iterative computation, the set of distances among the crystals can be resolved into a three-dimensional map of crystal position. This map is not in the observer's coordinate system; the coordinate system is determined by the positions of the first three crystals in the experiment. The first crystal is at the origin of the coordinate system. The second crystal is some distance along the x-axis, and the third crystal determines the x,y plane. (D) The effect of current flow on distance measurements. Sound will arrive at the receiving crystal faster when traveling in the direction of the flow. The sound pulse from crystal 1 to crystal 3 (blue arrow) would be speeded up, but the return pulse from crystal 3 to crystal 1 would be slowed down (red arrow). Cross-flow sound pulses, as from crystal 2 to crystal 1, would be unaffected (black arrow).

the skeletal elements involved in respiration, we used sonomicrometry, a well-established technique for measuring muscle shortening (Coughlin, 2000; Roberts et al., 1997; Shadwick et al., 1999). Sonomicrometry uses the time it takes an ultrasonic pulse to travel from one piezoelectric crystal to another to determine distance. The sonomicrometer used in these experiments is somewhat different from a conventional system in that each of the eight crystals acted as both a transmitter and a receiver (Fig. 1A,B), providing a total of 56 distance measurements (eight transmitters each with seven receivers) per polling cycle. This redundancy in measurements supposedly allows reconstruction of the crystal positions in three dimensions although, as we will discuss, this is quite difficult in practice. Sonomicrometry has notable advantages over other commonly used techniques for measuring the kinematics of internal structures: variable-inductance electrodes (i.e. Wainwright et al., 1995) and cineradiography (i.e. Liem, 1987). The inductance technique allows only one distance to be measured per experiment and reliably yields only relative distances. Cineradiography requires a large facility, does not work on uncalcified cartilaginous material and is impossible through an appreciable depth of water.

The hedgehog skate *Leucoraja erinacea* is an interesting model for examining water flow patterns and movements of the skeletal elements during respiration. Skates are extremely dorso-ventrally flattened elasmobranchs, with the mouth and gill slits on the ventrum, and the spiracle (an opening to the oropharyngeal cavity) on the dorsum. They typically breathe in through their mouth and spiracle and out through the gill slits (Hughes, 1960a; Rand, 1907). Skates spend much of their lives lying on the bottom, yet also swim actively during foraging and migration (Bigelow and Schroeder, 1953). This raises the possibility that they can employ more than one breathing mode, in that when they are buried they probably barely use their mouth and when swimming they might switch to breathing through the mouth. In addition, their ventrally directed mouth removes the complication of ram ventilation; they must power every respiratory cycle. Skate are well suited to respiratory experiments: they tend to stay on the bottom after surgery, their respiratory structures are easily accessed and they are large enough to allow sonomicrometry of the branchial structures.

We designed our experiments to answer three questions: (i) are the gill bars adducted during pressure reversals; (ii) is flow across the gills pulsatile, or does it oscillate; and (iii) is sonomicrometry a useful technique for determining kinematics in aquatic animals?

Materials and methods
Experimental animals

Adult hedgehog skates, *Leucoraja erinacea* (Mitchill), were captured by trawl in Frenchman Bay off Mount Desert Island, Maine, USA. They were transported to Mount Desert Island Biological Laboratory, Salsbury Cove, Maine, USA, and housed in a 3 m×4 m×0.4 m flow-through seawater tank (sex and size are given in Table 1). During their captivity, which varied from 1 to 3 months, they were fed an *ad libitum* diet of frozen shrimp and squid. Four adult hedgehog skates, either freshly frozen or fixed in formalin, were dissected to examine the putative water flow paths and the morphology of the plate-gills. These specimens remain in the private collection of A. P. Summers.

Fig. 2. Placement of sonomicrometry crystals (red) and pressure transducers (yellow) in the oropharyngeal and parabranchial chambers of the hedgehog skate *Leucoraja erinacea*. Water flow patterns (blue arrows) from one breathing mode (mode 1) are shown. Water flows into the spiracle, between the gill bars and out through the gill slits. In the cut-away of the parabranchial chamber, the fourth gill arch has been removed to show the morphology of the plate-like gills characteristic of elasmobranch fishes.
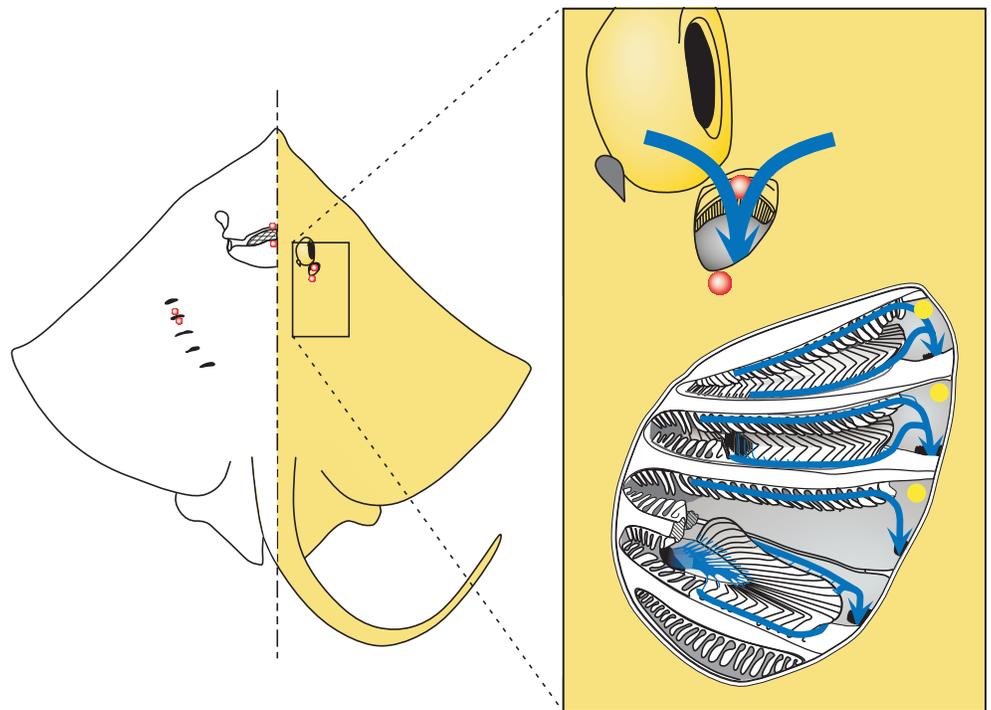
Sonomicrometry

We used an eight-channel digital sonomicrometer (Sonometrics Corp.) to measure the kinematics of eight key internal elements of the respiratory apparatus in 12 skates. To facilitate implantation, experimental animals were anesthetized in $0.133\,\mathrm{g\,l^{-1}}$ tricaine methanesulfonate (MS-222). At this time, the disk width was measured to the nearest 0.5 mm. Crystals were sutured inside the mouth to the upper and the lower jaw, the second and third gill bars, the skin over the spiracular cartilage, the edge of the spiracular opening and the anterior and posterior edges of the third gill slit (Fig. 2). All the crystals were 1 mm in diameter and attached to 38 gauge silver-plated copper wire, with the exception of the crystal on the edge of the spiracle, which was 2 mm diameter on 34 gauge wire. We experimented with 0.75 mm crystals, but the signal quality degraded significantly. The wires for the crystals implanted inside the oropharyngeal cavity were run through the floor of the oropharyngeal cavity, bundled with the wires running from the gill slit, sutured to the belly and led around the pelvic fin to the dorsal surface, where they joined the wires for the spiracular crystals. This bundle of wires was sutured to the skin over the spine; corks attached to the wire bundle kept it taut above the animal and floated it on the water.

Surgery lasted 20–45 min. Animals were then allowed to recover in the experimental chamber, a $28\,\mathrm{cm}\times28\,\mathrm{cm}\times104\,\mathrm{cm}$ acrylic aquarium maintained with flowing sea water at $11\pm0.5\,°\mathrm{C}$, for 1–2 h. After each experiment, the crystals were removed, cleaned and then re-used in the next surgery. Over the course of the 12 surgeries, three crystals stopped functioning and were replaced.

At least 10 sequences of 10 s of sonometric data were recorded over three or more hours following recovery. Data for the eight sonomicrometry channels were collected at 500 Hz with a transmit pulse of 500 ns and an inhibit delay of 3 mm. The system has an absolute error in measurement of 1.0 mm and a relative error of 0.0154 mm. In other words, the system can give the correct distance between two crystals to ±0.5 mm, and the distance measurement will be repeatable to 0.00752 mm. During data collection, the direction of water flow and closure of the oral and spiracular valves were confirmed by observing the movement of bubbles and particles in the water and of dye injected near these openings.

The data were filtered with a Sonometrics proprietary filtering program, Sonofilt. This software smoothes the data, corrects some signal level problems and makes a correction to the data that arises from different crystal diameters. The data were analyzed and filtered further using Sonosoft (Sonometrics Corp.). Sonosoft allowed us to remove or replace single data points that were obvious outliers from individual traces, to correct other signal level problems and to output an ASCII format data file suitable for use with Microsoft Excel.

Pressure

Pressure data were gathered simultaneously from the oropharyngeal and parabranchial chamber with two Millar Microtip SPC-330 pressure transducers. These are very high-frequency response (10 kHz) transducers sensitive to pressure changes as small as 0.133 Pa. Transducers were implanted into the chambers through PE 90 Intramedic polyethylene cannula tubing with a flange melted into one end. Each cannula was inserted through a 15 gauge hypodermic needle so that the flange pressed up against the inner wall of the oropharyngeal or parabranchial chamber; a ring of modeling clay pressed around the cannula on the external surface of the skate kept the tubing from dropping back into the chamber. After inserting the pressure transducer into the cannula, any air bubbles were purged from the cannula, and a second barrier of modeling clay sealed the gap between the transducer cable and the tubing and served to hold the transducer tip firmly in position at the margin of the inner wall of the oropharyngeal or parabranchial chamber. The oropharyngeal transducer was implanted lateral to the spiracle well posterior of the path of the hyomandibula. The parabranchial transducer was implanted at the lateral edge of the second or third chamber.

Pressure data were collected using the transducer bridge amplifiers. The analog signal was further amplified with a Tektronics direct current amplifier and both viewed and stored with the sonomicrometry data using the A/D channels of the Sonometrics board. The sampling rate for the pressure data was 500 Hz, the same as that of the sonomicrometry data. Before and after each experiment, the pressure transducers were calibrated at 25 and 23 cm of sea water to check for drift in the transducer amplifiers and the direct current amplifier. As long as the skate was nearly flat on the bottom of the tank, the two transducers were within 5 mm of the same depth, which we verified by checking the pressure while the skates were completely anesthetized.

Endoscopy

Three female skates were implanted with pressure transducers, as described above, and were additionally cannulated in the oropharyngeal and the parabranchial chambers with 1.1 mm internal diameter polyethylene tubing. A 1 mm diameter endoscope (Volpi Manufacturing), 75 cm in length, was inserted through these wider cannulae. Illumination was provided with an Intralux IK-1 fiber-optic light source, and images were recorded with a JVC DVL9800U digital camcorder attached to the eyepiece of the endoscope. It was not necessary to seed the water with particles to visualize flow because the unfiltered sea water contained plenty of suspended material. The pressure signal was used to modulate the frequency of an audible tone that was recorded by the microphone of the camcorder, allowing the pressure signals and video to be synchronized.

Analysis

The respiration rate for each breathing bout was measured as the number of complete respiratory cycles divided by time. Rate was measured for each respiratory mode that we identified, and for animals that had been implanted with sonomicrometry crystals as well as control animals that had only pressure transducers. Rate data for the two modes of

breathing that were well replicated among experimental animals (spiracle only and mouth+spiracle) were compared between the control and the implanted skate using a *t*-test. The maximum and minimum pressures generated in the oropharyngeal and parabranchial chambers were compared between these respiratory modes with simultaneous *t*-tests using a Bonferroni correction for multiple comparisons (Sokal and Rohlf, 1995).

We also analyzed the error inherent in the sonomicrometry data. We define the 'reciprocal' error of the sonomicrometry system as the difference between the distance measured from crystal a to crystal b and the distance measured from b to a. In a static system, with no water flow and simultaneous measurement of the a–b and b–a distance, the reciprocal error should be zero. This comparison was made for two crystal pairs from a normal (mouth+spiracle) breathing bout for three different animals. The difference between the measured distances is an error that affects accuracy.

Results

Respiratory modes and rates

During the experiments, the skate alternated between quiescent periods and periods of exercise in which they swam with varying degrees of vigor around the tank. This behavior appeared similar to that exhibited by the animals in the larger holding tanks with the exception that the swimming bouts were more frequent in the experimental tank. There were no attempts by the skate to rub the attached experimental apparatus off, to roll or to thrash about. Rather, the animal swam in a directed fashion around the tank, bumped into walls, swam up them and dropped back down to the bottom.

We were able to characterize five respiratory modes in the hedgehog skate, four in the experimental animals (Table 1) and a fifth mode in undisturbed animals. Note that these modes are not necessarily discrete behaviors but may be points along a continuum of respiratory response to activity level, stress or oxygen requirement. In any case, these five modes occurred frequently enough that we were able routinely to recognize them. Two of the five modes occurred with sufficient frequency to be analyzed quantitatively. The other three modes are described qualitatively but have not been subjected to analysis.

Mode 1: in through the spiracle only

The most common mode of respiration in quiescent animals involved pumping water in through the spiracle and out through the gill slits. Dye experiments showed that no water entered through the mouth although, from a sensory perspective, it is interesting that deformation of the nasal capsules during pumping was sufficient to draw water in through the anterior nasal opening. The dye then passed out of the nasal rosette *via* the posterior edge of the nasal curtain and along the underside of the animal to a point just lateral to the pelvic fin, where it left the body. This mode was observed in 10 of the 12 experimental animals and in several animals in the holding tank (Table 1).

Mode 2: in through the mouth+spiracle

This was seemingly a more energetic mode of respiration: water was pumped in through both the mouth and the spiracle and out through the gill slits. This mode was often seen after exercise and gradually gave way to the spiracle-only mode (mode 1). The skate often rose up slightly on its pectoral fins during this mode. Almost all experimental animals performed this mode of respiration for some period (Table 1).

Mode 3: in through the mouth only

The spiracle was held tightly closed and water was forcefully sucked in at the mouth and expelled from the gill

Table 1. *Experimental animals, implantation protocols and selected respiratory data for the hedgehog skate* Leucoraja erinacea

Skate	Sex	Disk width (cm)	Pressure	Kinematics				Mode*			
				Mouth	Gill bars	Spiracle	Gill slit	1	2	3	4
1	M	29.0	Ø	Ø	Ø	Ø	Ø	3	4		
2	M	28.0	Ø	Ø	Ø	Ø	Ø	5	2		
3	F	31.0	Ø	Ø	Ø	Ø	Ø	2	1		
4	F	31.5	X	X	X	X	X	2	3	3	
5	M	30.5	X	Ø	Ø	X	X	1	2		
6	F	31.0	X	X	X	X	X	5	1		
7	F	32.0	X	X	X	X	X	5			
8	F	30.5	X	X	X	X	X	5	2		
9	M	32.5	X	–	–	–	–		4		
10	F	32.0	X	–	–	–	–	2	2		
11	F	32.0	X	–	–	–	–	3	1		
12	F	31.5	X	X	Ø	X	X		3		2

*Number of times each respiratory mode was recorded. Mode 1, spiracle only; mode 2, mouth+spiracle; mode 3, mouth only; mode 4, mouth open throughout breathing cycle.

X indicates that kinematic or pressure data were gathered successfully; Ø indicates that, although the implantation was made, the data were not useful; a dash indicates that no implantation was made to gather data.

slits. This mode was seen in only one experimental animal (Table 1), but it lasted for over 15 min. It is unlikely that these data resulted from an insult to the spiracle because this behavior was seen between bouts of modes 1 and 2. As in the mouth+spiracle mode (mode 2), this occurred after a period of exercise.

Mode 4: mouth open throughout the respiratory cycle

Water was drawn in through the mouth and, while a substantial amount exited at the gill slits, there was also some flow out of the mouth. The mouth was not held widely open, but dye experiments showed that it was open far enough that the oral valve was not acting to prevent back-flow. This mode was observed in only one animal (Table 1), and it occurred after a very extended period of swimming around the tank. The skate was substantially raised up on its pectoral fins, and the flow volume out of the gill slits appeared to exceed that of the other modes we observed. It is worth noting that this mode has been observed in a round stingray (*Urolophus jamaicensis*) in the field by one of the authors (A.P.S.) after extensive attempts to capture the animal with a dip net while on SCUBA.

Mode 5: in and out through the spiracle

Undisturbed animals at rest on the bottom, for extended periods (greater than 1 min), breathe by pumping water in and out through the spiracle. This was not observed in animals that had been surgically implanted. During this mode, no water flow was observed at the mouth nor was there any flow out of the gill slits. In a shallow pan of water, prior to anesthesia, it was sometimes possible to see the surface of the water deformed by water exhaled from the spiracle. This mode was quite distinctive from the intermittent 'cough' that suddenly forced water out the spiracle and that could happen during any of the other respiratory modes.

A distinct coughing behavior, during which the oropharyngeal and parabranchial chambers were suddenly and forcefully compressed, was seen during all the breathing modes except mode 4. Coughs were highly variable and have not been analyzed kinematically. During a cough, the spiracle was always held open and the gill slits were passively opened by exhaled water; however, the mouth could be open or closed. Occasionally, a piece of visible detritus became stuck on the pseudobranch of the spiracle. This always elicited a coughing response within a few respiratory cycles.

During the experiments, the skate breathed continuously, with each complete breath taking approximately 2 s (Table 2). Implantation of sonomicrometry leads did not have an effect on the respiration rate compared with animals that had only the pressure cannulae ($t=1.24$, d.f.=25; $P=0.23$). Data were not collected on the respiratory rates of unoperated animals or from animals in the wild, but our impression is that the experimental rates were slightly higher. The animals without the sonomicrometry implants only exhibited two of the four respiratory modes that we saw in the other experimental animals. This is not unexpected because the rate of occurrence of modes 3 and 4 was very low (Table 1).

Kinematics and pressure

Nine of the 12 animals with pressure transducers yielded clean data that did not require filtering. Thus, the pressure and sonometric data presented are primarily from these animals. The sonomicrometry data were extremely clean between adjacent crystals (i.e. crystals 1–2, 3–4, etc.) in the individuals that were implanted (Table 1). However, there was considerable noise between other crystal pairs, and on many occasions non-adjacent crystals did not yield useable data. This, in combination with distance measurement errors related to flow (see Discussion), made reliable three-dimensional reconstruction of the crystal positions impossible. In this paper, we have used only linear distances, as measured between adjacent crystals. Linear distances were usually computed as the average of the two distances measured between each crystal pair. However, in a few cases, a crystal was able to send a good signal but not receive one. For these crystals, there is only a single distance measurement.

Data for the two frequently occurring respiratory modes, spiracle only (mode 1) and mouth+spiracle (mode 2) were examined separately.

Mode 1: spiracle only

Pressure in the oropharyngeal cavity oscillated between −32.8 Pa and +169 Pa relative to ambient, while pressure in the parabranchial chambers ranged from −51 Pa to +73 Pa (Table 3). Although there was no flow into the oropharyngeal

Table 2. *Respiratory rates of the hedgehog skate* Leucoraja erinacea

Mode	Sonomicrometry implant (Hz)	Pressure only (Hz)	No manipulation
Spiracle only	32.4±6.0 (28)	30.6±7.8 (5)	
Mouth+spiracle	33.0±10.2 (15)	43.8±8.4 (7)	
Mouth only	27.6±1.8 (5)		
Mouth open (in and out)	18±3.6 (5)		
Hughes (1960a)		37.8 (1 fish)	
Rand (1907)			45.6±8.4 (5) (5 fish)

Values are means ± S.D. (*N*).

Table 3. *Pressures from the oropharyngeal and parabranchial chambers of the hedgehog skate* Leucoraja erinacea

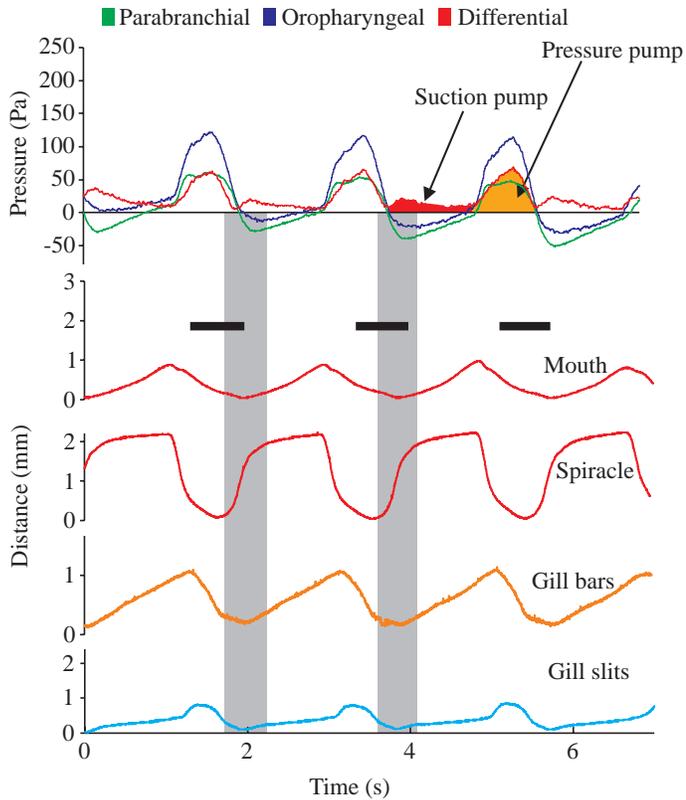|	Oropharyngeal pressure (Pa)		Parabranchial pressure (Pa)	
	Maximum	Minimum	Maximum	Minimum
Spiracle only	169±37	−32.8±11	73±11	−51±10
Mouth+spiracle	204±17	−86±10	146±12	−74±9

Values are means ± S.D. (*N*=42).

Fig. 3. Kinematic and pressure traces from a hedgehog skate *Leucoraja erinacea* breathing in through the spiracle and out through the gill slits (mode 1) showing both pressure pump and suction pump phases. The pressure graphs show the oropharyngeal and parabranchial pressure as well as the pressure differential between these two cavities. A positive pressure differential indicates that there is a higher pressure in the oropharyngeal cavity than in the parabranchial chambers. The vertical gray columns indicate periods when the gill bars are adducted. The red filled region on the pressure trace indicates the suction pump period. The orange filled region on the pressure trace and the black horizontal bars on the kinematic trace indicate the compressive, or pressure pump, phase of the respiratory cycle. The crystals on the gill bars were sutured to the center of the gill bars, so even when they were fully closed there was still some distance between them. For this reason, the distance between them never reaches zero.
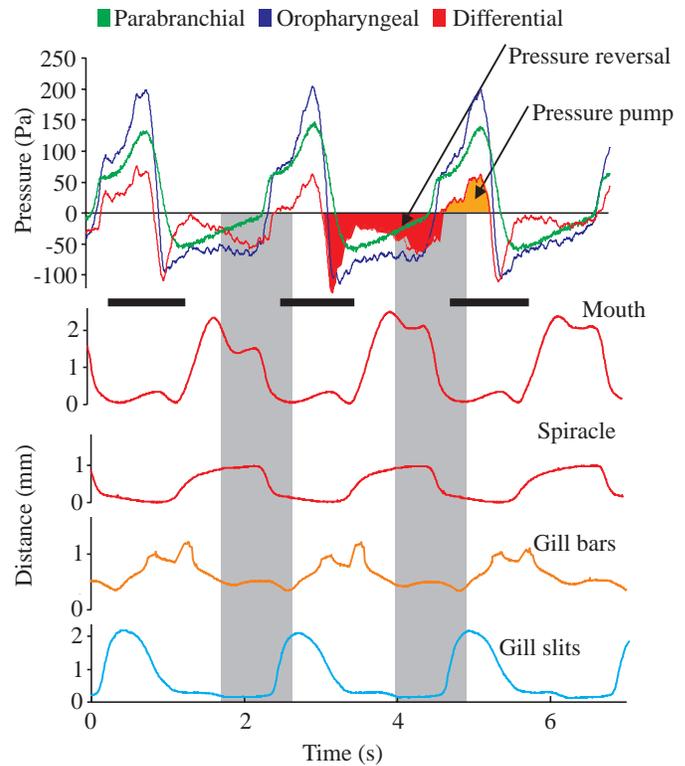
Fig. 4. Kinematic and pressure traces from a hedgehog skate *Leucoraja erinacea* breathing in through both the mouth and spiracle and out through the gill slits (mode 2), showing that there is a pressure pump phase only. The pressure graphs show the oropharyngeal and parabranchial pressures as well as the pressure differential between these two cavities. A positive pressure differential indicates that there is a higher pressure in the oropharyngeal cavity than in the parabranchial chambers. A negative pressure, or pressure reversal, is indicated by the red region. The vertical gray columns indicate periods when the gill bars are adducted. The orange filled region on the pressure trace and the black horizontal bars on the kinematic trace indicate the compressive, or pressure pump, phase of the respiratory cycle.

cavity through the mouth, the upper and lower jaws were drawn apart in rhythmic fashion in time with the opening of the spiracles. It appeared that soft tissue around the oral opening served as a valve and prevented water from entering. The gill bars were abducted cyclically as well, with maximum obstruction of the passage from the oropharyngeal to the parabranchial chamber occurring while the gill slits were maximally open (Fig. 3).

Mode 2: mouth+spiracle

Pressure in the oropharyngeal cavity oscillated between −86 Pa and +204 Pa relative to ambient (Table 3). This is significantly higher than the maximum oropharyngeal pressures seen during spiracle breathing (t=3.7, d.f.=40,

P<0.01) and significantly lower than the minimum pressures (t=−16.0, d.f.=40, P<0.01). Pressure in the parabranchial chambers ranged from −74 Pa to +146 Pa, which is significantly higher than the maximum parabranchial pressures seen during spiracle breathing (t=26.9, d.f.=40, P<0.01) and significantly lower than the minimum pressures (t=8.02, d.f.=40, P<0.01). The kinematics of the spiracle and the mouth shows similar patterns in terms of the timing of opening and closing (Fig. 4). The opening of the gill slits is 180° out of phase with that of the spiracle and mouth. The pressure profile reveals periods when the pressure in the parabranchial chambers exceeded the pressure in the oropharyngeal cavity, i.e. a pressure reversal. The maximal closure of the gill bars is coincident with the majority of these periods (Fig. 4).

Water flow

During endoscopy, the mouth+spiracle mode was the only

mode of breathing we observed. The endoscope showed that water flow was not continuous on the oral side of the gill bars and on the parabranchial side. From the oral side, water flowing into the primary lamellae stopped and reversed direction with every breathing cycle. From the parabranchial side, water flow from between the primary lamellae was pulsatile, with flow frequently stopping and sometimes also reversing direction. This was most clearly seen at the gill bars and in the circumferential canal of the parabranchial chamber. The reversals were smaller in magnitude immediately next to the outflow of the primary lamellae.

We are unable to present quantitative data on flow as seen through the endoscope for several reasons. The lens of the endoscope yielded a distorted image (due to curvature) that was unsuitable for estimating distances or velocities. Furthermore, it was our impression that the flow field was variable depending on where the endoscope was pointing. We would expect that in some regions of the gill the flow stops while in other regions it reverses direction, and it was not possible to precisely standardize implantations among animals. The qualitative data, however, are unequivocal as to the repeated presence of stopped and/or reversed flow. The endoscopic data are consistent with the pressure data such that the pressure data can be used as a rough proxy for flow in this system. While a negative pressure, or pressure reversal, does not necessarily mean that a flow reversal has occurred, we have verified, at the very least, that a flow stoppage will occur.

Reciprocal error

The reciprocal error measured between the anterior gill bar and posterior gill bar crystals was 0.15 ± 0.06 mm (mean $\pm$ S.D.). There was no dependence of the error on the distance between the crystals, but the error did show discrete jumps from one value to the next that corresponded to the distance resolution of the system. The reciprocal error measured between the upper jaw and posterior gill bar crystals was 0.18 ± 0.03 mm and showed what appeared to be a strong dependence on the distance between the two crystals. This was determined to be an artifact of flow between the crystals and was confirmed by a haphazard sample of the reciprocal error of other crystals pairs.

Discussion

Constant countercurrent flow?

The hedgehog skate exhibited several modes of ventilation, and two were observed with sufficient frequency to be analyzed thoroughly and appear to be common in the ventilatory repertoire of the species. They were taking in water through the spiracle only (mode 1) and taking in water by the combined actions of the mouth and spiracle (mode 2).

During the spiracle-only mode of breathing, there is an effective pressure pump (Fig. 3), a period when the pressure in the oropharyngeal cavity is much greater than the pressure in the parabranchial cavity. During this phase, water is presumably forced from the oropharyngeal to the parabranchial cavity by the pressure difference (Ferry-Graham, 1999; Hughes, 1960a; Liem et al., 1985). There is also an effective suction pump, a period when pressure in the oropharyngeal cavity is negative relative to ambient, but pressure in the parabranchial cavity is even more negative. During this phase, water is sucked from the oropharyngeal to the parabranchial cavity (Fig. 3). This would suggest that water is continually flowing over the gills in an anterior to posterior fashion, as predicted by early models of fish respiration (Hughes and Ballintijn, 1965; Hughes and Morgan, 1973). However, it should be noted in Fig. 3 that the gill bars do actively abduct and adduct during ventilation. This means that there is a period during which water flow over the gills is slowed or stopped by the closed gill bars. If water flow over the gills is merely slowed by the abduction and adduction of the gills, the flow of water is continuous during this breathing mode, but it is not of constant velocity. If water flow over the gills is stopped by their movements, flow cannot be considered to be continuous.

For mouth+spiracle breathing, a pressure pump was detected (Fig. 4), but no suction pump was seen. Pressure reversals were evident (Fig. 4), i.e. periods during which the pressure differential was negative and water would be forced from the parabranchial to the oropharyngeal cavity. The reversals, however, generally coincided with the adduction of the gill bars, so they could prevent, or at least attenuate, back-flow. Fortunately, we were able to supplement the kinematic and pressure data from this breathing mode with visual data from the endoscope. The endoscopic data reveal that the adduction of the gill bars does not completely prevent the back-flow of water during the pressure reversals. The flow of water during this respiratory mode is presumably at some times counter-current and at some times co-current with the flow of blood through the gills.

Counter- versus co-current gas transfer and continuous flow over the gills

Models of gas transfer across fish gills serve two purposes: (i) they allow comparison of oxygen uptake efficiencies that are based on the morphology of the gill rather than invasive physiological experiments; and (ii) the impact of the variable morphological characteristics of the gill on oxygen uptake efficiency can be evaluated (Piiper, 1989). An assumption of gas transfer models is that the flow of water is counter-current with respect to the blood flow and that it is of constant speed (Piiper, 1998; Piiper and Scheid, 1984). There is good experimental evidence against the existence of a completely co-current flow of water over the gills (Grigg and Read, 1971; Hills and Hughes, 1970; Piiper and Baumgarten-Schumann, 1968b). In a conventional co-current system, the O_2 content of newly oxygenated blood can be no higher than the O_2 level of the water that is flowing out of the gill. In contrast, in a counter-current system, the O_2 content of the oxygenated blood is limited by the O_2 level of the water flowing into the gill. Complicated variations on the co-current theme have been proposed (Piiper and Schumann, 1967), but none approaches the extraction efficiency of a counter-current system (Grigg

and Read, 1971). Direct measurements in bony and cartilaginous fishes have found the O_2 content of the oxygenated blood to be far higher than that of the expired water (see, for example, Azuma and Itzawa, 1993; Piiper and Baumgarten-Schumann, 1968a; Smatresk, 1986). This has been interpreted as evidence for a counter-current system, but really it is evidence against a purely co-current system.

The other assumption, that of constant flow velocity, is not well supported by current experimental evidence. The variable flow field was recognized but dismissed as unimportant in early analyses of gill function (Hughes and Morgan, 1973). More recently, models have quantified the effect of variable-speed, unidirectional flow on oxygen extraction efficiency (Malte, 1989). That study found that the penalty for pulsatile flow varied for different species, with fast-swimming species suffering the greatest degradation in oxygen extraction efficiency (10–25 %) while the catshark *Scyliorhinus canicula* was relatively unaffected (3 % reduction). The models used to generate the estimates of relative efficiency used a sine wave to represent changing flow velocity. Our pressure profiles indicate that a more complicated curve would be appropriate, and the statement of the model is such that substituting another curve would be relatively simple. However, there is no simple way to adapt the models of Malte (1989) to account for an actual flow reversal. The difficulty lies is setting the boundary conditions during the simulation. Determining the effect of flow reversals will require a new generation of theoretical models.

On the applicability of sonomicrometry for measuring kinematics

Sonomicrometry would seem ideally suited to determining the kinematics of the respiratory system of a skate. There are well-known problems associated with using this technique close to airspaces and surfaces with high sound reflectance such as bone. However, neither of these applies to fishes existing completely under water and with a cartilaginous skeleton. Nevertheless, we were unable to reconstruct three-dimensional data with any confidence using the system. In the process of troubleshooting our system, and in designing an application for bony fishes, we have identified several issues that should be considered when using sonomicrometry to reconstruct kinematics.

The Sonometrics system polls each of the crystals in turn, so there is a delay between the measurement of the distance from a to b and the distance from b to a. Furthermore, this delay is related to how far apart the crystals are in the polling cycle. In a system sampling at 250 Hz, numerically adjacent crystals (i.e. 4 and 5 or 7 and 8) have only a 0.004 s delay, whereas crystals four places apart in the cycle array (i.e. 1 and 5 or 3 and 7) have a 0.016 s delay. This delay has little effect when the elements to which they are attached are not moving quickly. However, a crystal attached to a fast-moving element, such as the protruding upper jaw of a teleost fish, might move several millimeters in 16 ms. The polling issue adds a speed-dependent error to reconstruction of three-dimensional

kinematics because the reconstruction algorithm treats a set of distance data as having been captured at a single instant in time.

An additional source of disagreement between the distance measured from a to b and the distance from b to a is caused by a threshold error. When an ultrasonic pulse arrives at a crystal, it is not recognized until the sound pressure reaches some threshold amplitude above the ambient noise level. Setting this threshold is an important part of ensuring clean distance measurements. The leading edge of the ultrasonic pulse is steep but not vertical. Changing the recognition threshold changes the time at which the software perceives a pulse because the pulse is sampled at a different place on the leading edge. Thresholds are set separately for each crystal and seem to be highly dependent on the precise placement of the crystal, i.e. they vary from experiment to experiment even though the crystals are nominally in the same place. So, crystal **a** might recognize a sound pulse several microseconds after crystal **b**. In practice, this leads to a small, system-wide reciprocal distance error.

The most perplexing error we encountered was a fluid-velocity-dependent discrepancy between reciprocal pairs. This is important only when there is significant flow parallel to a line between two crystals, but it is a troublesome error when it occurs because it is of variable and unpredictable magnitude. An ultrasonic pulse will travel faster in the direction of flow than against it. A continuous flow bias could be accounted for by averaging the reciprocal distances, but flow that varies cyclically introduces an error that is difficult to correct. In Fig. 5A, we show reciprocal error between crystals that have transverse flow between them, while the crystals in Fig. 5B see cyclical flow. The error in Fig. 5B appears to depend on the distance between the two crystals. However, it is slightly out of phase with distance and, rather than being symmetrical in shape, the rising wave is far less steep than the falling wave. It is worth noting that this is in no way a design flaw. In fact, if the crystals are constrained not to move relative to one another, they will form a non-contact flow meter. These errors make the reconstruction of three-dimensional crystal position very unreliable in our experiment, where there are pulsatile flows in several, unpredictable directions.

There is a further difficulty with the general task of three-dimensional reconstruction that was not obvious at the beginning of this experiment. The problem lies in establishing a frame of reference. The sonomicrometry crystals are not able to locate themselves in the viewer's frame of reference, nor in any other external frame. So, any three-dimensional reconstruction has to begin by establishing a sonomicrometry crystal frame of reference; this requires an origin (0,0,0) and a plane through this point. Establishing the origin comes down to holding the position of one crystal (i.e. crystal 1) completely fixed and allowing the others to move relative to it. Specifying the plane constrains the motion of two other crystals (i.e. crystals 2 and 3), which cannot be co-linear with the origin crystal. Crystal 2 is constrained to move back and forth along a line drawn
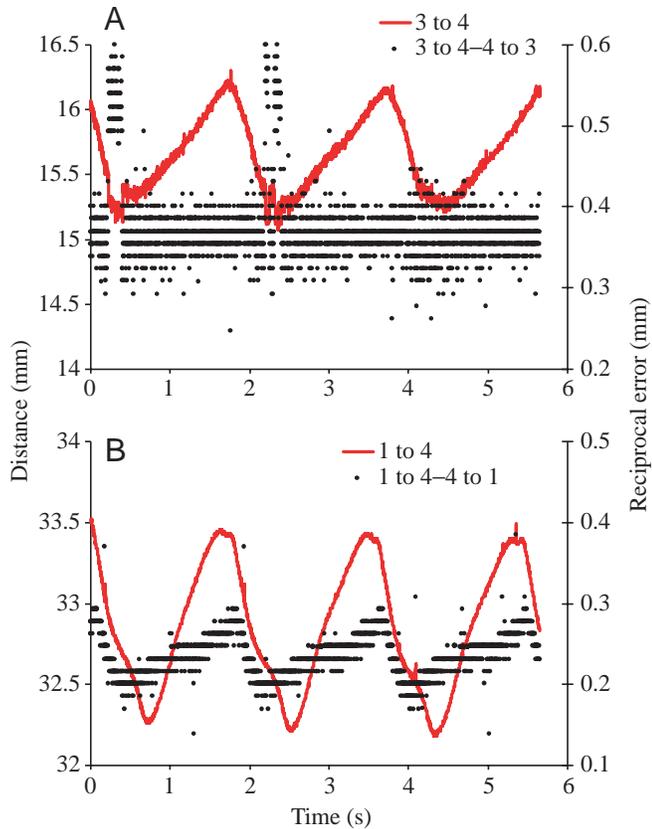
Fig. 5. An example of the reciprocal distance error in sonomicrometry when used to determine kinematics in a region with moving fluid. Two distances are generated for each crystal pair: from a to b and from b to a. These plots show the raw distance between two crystals (i.e. from a to b) (left-hand y-axis) and the difference between this distance and the reciprocal distance (i.e. a to b minus b to a) (right-hand y-axis). (A) The distance between the pair of crystals located on adjacent gill bars. The water flow in this area is perpendicular to a line between the two crystals. The reciprocal error is not related to the distance between the crystals. (B) The distance between the pair of crystals located on the upper jaw and the posterior gill bar. The water flow in this region is cyclical and parallel to a line drawn between the crystals. The reciprocal error is strongly dependent on the velocity of water between the two crystals. The error is slightly out of phase with the actual distance measurement, and the shapes of the curves are different.

between it and the origin crystal, effectively becoming the x-axis of the plane. Crystal 3 cannot be on the line between crystals 1 and 2, and with crystal 2 serves to define an x,y plane that passes through the origin (see Fig. 1C). All other movements of these three crystals in the observer's frame of reference are added into the motions of the remaining crystals. Three-dimensional reconstructions are viewed by the observer in the frame of reference of the crystal, which is constantly moving with respect to the frame of reference of the observer.

The solution to this difficulty is to have three crystals that do not move at all with respect to each other and occupy defined anatomical positions. This allows the simple construction of a transformation from the frame of reference

of the user to the sonomicrometry frame of reference. Alternatively, the three reference crystals could be physically constrained to be coplanar, and ideally crystal 1 would be motionless and crystal 2 would move back and forth along a well-understood path. Fixing the positions of three crystals represents a large overhead in an eight- or 16-crystal system. Furthermore, it is unclear where three such crystals can be placed within the head of a fish. Very few anatomical elements remain motionless or move solely along one axis. Yet, the crystal must be placed within the fish for the remaining calculations of three-dimensional movements to be in the fish frame of reference.

The reconstruction of the three-dimensional kinematics of internal structures is an incredibly powerful tool for functional morphologists, and there are very few ways that it can be done. Sonomicrometry is not an ideal solution, but the difficulties and errors are not insurmountable and the technique has great potential in certain situations.

Respiration in cartilaginous fishes

We have demonstrated that there are intricacies to respiration in cartilaginous fishes that are not addressed by current models of gas transfer. Two areas that we feel are particularly worth pursuing are the role of the spiracle in respiration and the effect of multiple gill chambers on respiratory function. The spiracle, the dorsal opening into the oropharyngeal cavity, is of very variable character. Several families of shark have lost it completely; others have a spiracle, but no valve to close it; still other groups have large, valved spiracles that seem to be important in respiration. This additional opening into the oropharyngeal chamber may play an important role in some aspects of respiration.

There is some indication that the subdivisions of the parabranchial chambers, each of which has its own gill slit, receive different water flow and have different oxygen extraction efficiencies (Ballintijn, 1972; Piiper and Schumann, 1967). This possibility has several ramifications: it may lead to differing oxygen levels in afferent arteries, it might represent a reservoir of pumping potential for periods of high exercise, or it could be an indication that some gill arches are becoming relictual. It is interesting to note that the ram-ventilating, fast-swimming sharks have only five gill slits and no spiracle, in contrast to the six or seven gill slits of slower-swimming sharks and rays (Compagno, 1984).

References

Azuma, T. and Itzawa, Y. (1993). Respiration of a marine teleost, the porgy, under normoxic, resting condition. *Nippon Suisan Gakkaishi* **59**, 621–626.

Ballintijn, C. M. (1969). Functional anatomy and movement co-ordination of the respiratory pump of the carp (*Cyprinus carpio* L.). *J. Exp. Biol.* **50**, 547–567.

Ballintijn, C. M. (1972). Efficiency, mechanics and motor control of fish respiration. *Respir. Physiol.* **14**, 125–141.

Bigelow, H. B. and Schroeder, W. C. (1953). Sawfishes, guitarfishes, skates and rays. In *Fishes of the Western North Atlantic*, vol. 1, part 2 (ed. J. Tee-Van), pp. 1–514. New Haven, CT: Sears Foundation for Marine Research.

Compagno, L. J. V. (1984). *Sharks of the World – An Annotated and Illustrated Catalogue of Shark Species Known to Date*. New York City: United Nations FAO Guide.

Coughlin, D. J. (2000). Power production during steady swimming in largemouth bass and rainbow trout. *J. Exp. Biol.* **203**, 617–629.

Ferry-Graham, L. A. (1999). Mechanics of ventilation in swellsharks, *Cephaloscyllium ventriosum* (Scyliorhinidae). *J. Exp. Biol.* **202**, 1501–1510.

Grigg, G. C. and Read, J. (1971). Gill function in an elasmobranch. *Z. Vergl. Physiol.* **73**, 439–451.

Hills, B. A. and Hughes, G. M. (1970). A dimensional analysis of oxygen transfer in the fish gill. *Respir. Physiol.* **9**, 126–140.

Hughes, G. M. (1960a). The mechanism of ventilation in the dogfish and skate. *J. Exp. Biol.* **37**, 11–27.

Hughes, G. M. (1960b). A comparative study of gill ventilation in marine teleosts. *J. Exp. Biol.* **37**, 28–45.

Hughes, G. M. and Ballintijn, C. M. (1965). The muscular basis of the respiratory pumps in the dogfish (*Scyliorhinus canicula*). *J. Exp. Biol.* **43**, 363–383.

Hughes, G. M. and Morgan, M. (1973). The structure of fish gills in relation to their function. *Biol. Rev.* **48**, 419–475.

Hughes, G. M. and Shelton, G. A. (1958). The mechanism of ventilation in three freshwater teleosts. *J. Exp. Biol.* **35**, 807–823.

Lauder, G. V. (1980). The suction feeding mechanism in sunfishes (*Lepomis*): an experimental analysis. *J. Exp. Biol.* **88**, 49–72.

Liem, K. F. (1987). Functional design of the air ventilation apparatus and overland excursions by teleosts. *Field. Zool.* **37**, 1–29.

Liem, K. F., Wallace, J. W. and Whalen, G. (1985). Flatfish breathe symmetrically: an experimental reappraisal. *Exp. Biol.* **44**, 159–172.

Malte, H. (1989). Pressure/flow relations in the interlamellar space of fish gills: theory and application to the rainbow trout. *Respir. Physiol.* **78**, 229–242.

Piiper, J. (1989). Factors affecting gas transfer in respiratory organs of vertebrates. *Can. J. Zool.* **67**, 2956–2960.

Piiper, J. (1998). Branchial gas transfer models. *Comp. Biochem. Physiol.* **119**A, 125–130.

Piiper, J. and Baumgarten-Schumann, D. (1968a). Transport of O_2 and CO_2 by water and blood in gas exchange of the dogfish (*Scyliorhinus stellaris*). *Respir. Physiol.* **5**, 326–337.

Piiper, J. and Baumgarten-Schumann, D. (1968b). Effectiveness of O_2 and CO_2 exchange in the gills of the dogfish (*Scyliorhinus stellaris*). *Respir. Physiol.* **5**, 338–349.

Piiper, J. and Scheid, P. (1984). Model analysis of gas transfer in fish gills. In *Fish Physiology*, vol. XA (ed. W. S. Hoar and D. J. Randall), pp. 229–262. Orlando, FL: Academic Press.

Piiper, J. and Schumann, D. (1967). Efficiency of O_2 exchange in the gills of the dogfish, *Scyliorhinus stellaris*. *Respir. Physiol.* **2**, 135–148.

Rand, H. W. (1907). The functions of the spiracle of the skate. *Am. Nat.* **41**, 287–302.

Roberts, T. J., Marsh, R. L., Weyand, P. G. and Taylor, C. R. (1997). Muscular force in running turkeys: The economy of minimizing work. *Science* **275**, 1113–1115.

Sanderson, S. L., Stebar, M. C., Ackermann, K. L., Jones, S. H., Batjakas, I. E. and Kaufman, L. (1996). Mucus entrapment of particles by a suspension-feeding tilapia (Pisces: Cichlidae). *J. Exp. Biol.* **199**, 1743–1756.

Scheid, P. and Piiper, J. (1976). Quantitative functional analysis of branchial gas transfer: Theory and application to *Scyliorhinus stellaris* (Elasmobranchii). In *Respiration of Amphibious Vertebrates* (ed. G. M. Hughes), pp. 17–38. New York: Academic Press.

Shadwick, R. E., Katz, S. L., Korsmeyer, K. E., Knower, T. and Covell, J. W. (1999). Muscle dynamics in skipjack tuna: timing of red muscle shortening in relation to activation and body curvature during steady swimming. *J. Exp. Biol.* **202**, 2139–2150.

Smatresk, N. J. (1986). Ventilatory and cardiac reflex responses to hypoxia and sodium cyanide in *Lepisosteus osseus*, an air-breathing fish. *Physiol. Zool.* **59**, 385–397.

Sokal, R. R. and Rohlf, F. J. (1995). *Biometry*. New York: W. H. Freeman & Company.

Wainwright, P. C., Turingan, R. G. and Brainerd, E. L. (1995). Functional morphology of pufferfish inflation: mechanism of the buccal pump. *Copeia* **1995**, 614–625.